

Absorption Coefficient in a MQW Intersubband Photodetector with Non-Uniform Doping Density & Layer Distribution

Kasturi Mukherjee^{1, *} and Nikhil R. Das²

Abstract—Selective wavelength tuning of multiple quantum well based infrared photodetector is achieved by non-uniform doping distribution as well as dimensional variation in the structure. Result is obtained from the computation of the intersubband transition energy through self-consistent solution of the Poisson's and Schrödinger equations with appropriate boundary conditions. Absorption coefficient is estimated in presence of external electric field applied along the direction of confinement. Suitable choice of structural parameters is required to tailor the peak position of absorption spectra for application in the infrared range as optical receiver.

1. INTRODUCTION

Bandgap engineering in quantum heterostructures has attracted researchers to focus their application on optoelectronic devices in infrared range [1]. Quantum well provides one-dimensional confinement to the motion of the charge carriers which leads to their quantization of energy. The position of the discrete energy levels in the conduction and valence band quantum wells is controlled by the thickness of the well and the surrounding barrier layer, quantum well doping density and material composition regulating the band-offset [2, 3]. The variation in the structural parameters or the externally applied bias or appropriate combination of both can tune the energy subband positions and consequently the intersubband gap in the well to tailor the effective band gap in nanostructures in contrary to the fixed band gap in bulk counterparts. Researchers have utilized this novel feature to design intraband or intersubband photodetectors using multiple quantum well structures for color spectra detection that overcome the limitation of monochromatic wavelength absorption by traditional bulk interband photodetectors [4–6]. In recent days Quantum Well Infrared Photodetectors (QWIPs) are widely used for short, mid, long and very-long wavelength infrared detection, thermal imaging, medical imaging and many other real life applications [7–9]. The impact of number of wells, doping density, applied bias and position of quasi-bound states on the operating wavelength and other performance parameters of the intersubband QWIPs have been reported by the researchers for multifarious applications [10–13]. The dark current, photocurrent and detectivity of the multiple well infrared detectors with asymmetric barrier layer and stepped well design have also been investigated [14–16]. However, according to the knowledge of the authors, the study of the absorption coefficient with non-uniformity in dimensional as well as structural parameters in multiple quantum well based optical receiver is not paid attention to so far. In this paper, focus is made on the theoretical analysis of the absorption coefficient in non-uniformly wide and doped multiple quantum well intersubband photodetectors and hence, the choice of structure appropriate for application in the infra-red range is extracted.

The remaining sections of this article are organized as follows. The theoretical calculations involving the self-consistent solution of Schrödinger and Poisson's equations are shown in details in Section 2. The results and relevant explanations are given in Section 3. Finally, a conclusion is given in Section 4.

Received 19 August 2014, Accepted 19 September 2014, Scheduled 26 September 2014

* Corresponding author: Kasturi Mukherjee (kaskedar.mk@gmail.com).

¹ Heritage Institute of Technology, Kolkata, India. ² Institute of Radio Physics & Electronics, University of Calcutta, India.

2. THEORY

We consider a multiple quantum well (MQW) structure consisting of doped quantum wells and undoped barriers grown along the direction of confinement and the rightmost contact end, i.e., collector region is positively biased with respect to the emitter region in the leftmost contact end. The absorption coefficient peak position corresponding to the incident photon wavelength depends on the subband energy position and intersubband energy difference in the wells at a particular applied bias. In order to compute the coefficient Schrödinger and Poisson's equations are solved self-consistently by analytical means.

The time-independent Schrödinger equation in a well (say, r th well) belonging to the MQW structure subjected to externally applied bias is given by Eq. (1),

$$-\frac{\hbar^2}{2m^*} \frac{d^2\psi}{dx^2} + [V_W - qF(x)x] \psi(x) = E\psi(x) \quad (1)$$

where, \hbar is the reduced Planck's constant, m^* the effective mass of electrons, q the electronic charge, F the electric field in the r -th region, V_W the potential energy at the left end of the first quantum well from the emitter end, $\Psi(x)$ the wave function, and E the total energy of the electron. Solution of the Poisson's equation (Eq. (2)) taking into account the ionized donor density ($N_{D,well,r}^+$) and free electron concentration (n_r) in the quantum well gives the field F in this region (say, r -th well) as given below,

$$\frac{dF}{dx} = \frac{q(N_{D,well,r}^+ - n_r)}{\epsilon_r} \quad (2)$$

The self-consistent calculation begins with the solution of Eq. (1) for the computation of eigen energies in the quantum wells at zero bias for specified well width and well doping density. The internal electric field due to doping in the well layer causes band bending of the MQW structure even when it is unbiased to attain Fermi-level alignment throughout the structure.

With the application of external voltage, the electric field and hence, the tilting of the energy band profile is further modified which aids in the thermionic emission of electrons from the quantum wells varying the free electron concentration in this layer and, this, in turn again influences the subband energy positions through band-offset profile. So, Eqs. (1) and (2) are solved self-consistently to accurately calculate the energy subbands in the quantum wells. For a given applied bias, the effective electric field in different well and barrier layers are found by summing the field due to external voltage and that due to doping distribution in the corresponding regions. The energy subbands at this bias is evaluated from the solution of Eq. (1).

The effective number of electrons (N_{th}) coming out of the quasi-bound states in the quantum wells via tunneling assisted thermionic emission is obtained from Eq. (3) [17],

$$N_{th}(E_j) = \left(\frac{m^*}{\pi \hbar^2 (L_w + L_b)} \right) \int_{E_j}^{\infty} f(E) \mathfrak{S}(E) dE \quad (3)$$

where, E_j is the j -th subband in a well, L_b the barrier width, L_w the well width, $f(E)$ the Fermi-Dirac distribution function, and $\mathfrak{S}(E)$ the transmission coefficient of electrons tunneling through neighboring barrier layer.

Considering the variation of free electron concentration in the quantum well because of the above mentioned process, the modified value of the average electric field in the first quantum well is calculated from Eq. (4),

$$F_{W,1}^{Avg} = F_{W,1}^i + \frac{q (N_{D,well,1}^+ - n_1) L_{w,1}}{2\epsilon_w} = F_{W,1}^U \quad (4)$$

The new electric field distribution ($F_{W,k}^U$) obtained in the other quantum wells (say, k -th well) except the first well near the emitter end through iterations of the self-consistent solution is expressed in a generalized manner as follows,

$$F_{W,k}^U = \left[F_{W,1}^i + \frac{q}{2\epsilon_w} \left\{ (N_{D,well,k}^+ - n_k) L_{w,k} + \sum_{r=1}^{k-1} 2 (N_{D,well,r}^+ - n_r) L_{w,r} \right\} \right] \quad (5)$$

The calculations from Eqs. (1)–(5) are iterated until the condition of convergence is satisfied ($|\frac{F_{W,1}^U - F_{W,1}^i}{F_{W,1}^i}| < 10^{-4}$) to calculate near accurate position of energy subband(s) in the quantum well. The flowchart representation of the iterative procedure described here is given in Figure 1. The accurate intersubband energy gap is subsequently computed using simple arithmetic.

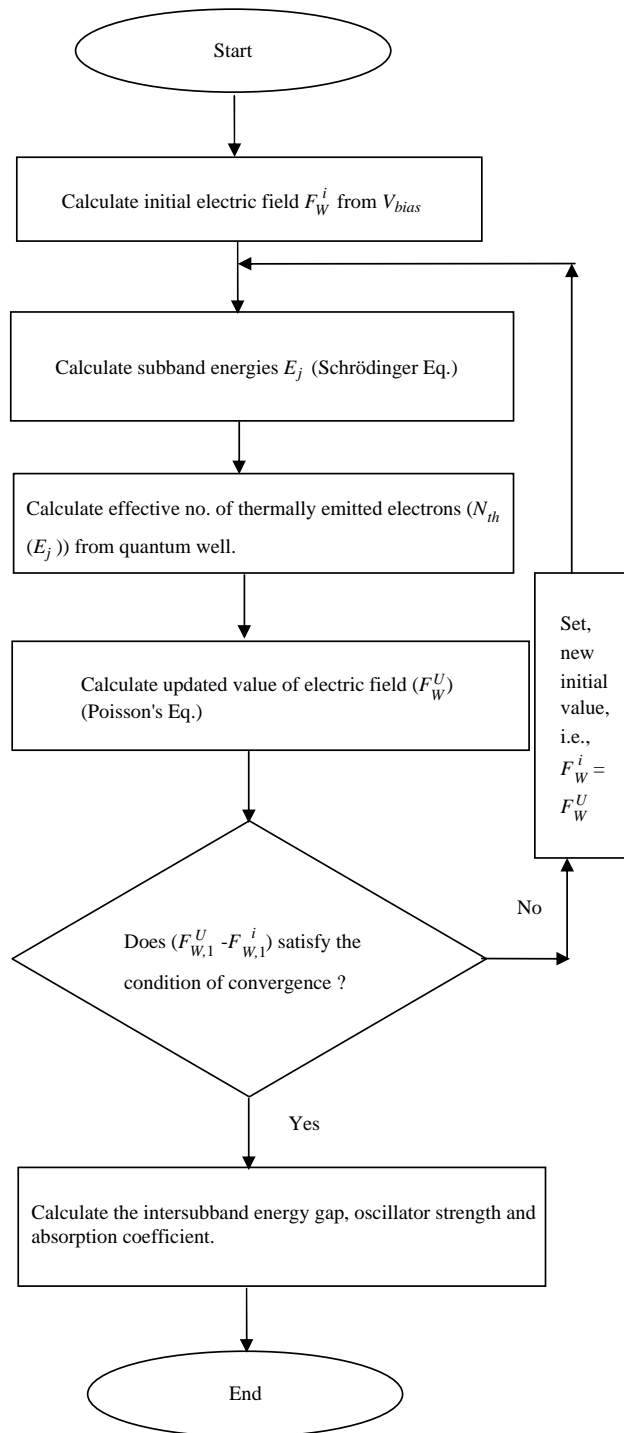


Figure 1. Flowchart representing the self-consistent iterative procedure of solution of the Schrödinger and Poisson’s equations to calculate the absorption coefficient in a multiple quantum well structure.

The oscillator strength of intersubband absorption in the quantum well for the incident photon energy ($\hbar\omega$) is estimated using Eq. (6) [17],

$$f_{jf} = \frac{2m^*\omega}{\hbar} |\langle \psi_j | x | \psi_f \rangle|^2 \quad (6)$$

The intersubband absorption coefficient of the multiple quantum well infrared photodetector primarily depends on the momentum matrix element, difference in the subband density of electrons in the ground and the excited state and the incident radiation wavelength as mentioned in Eq. (7),

$$\alpha(\omega) = \left\langle \sum_{r=1}^{N_W} \frac{\pi q^2 \hbar}{\varepsilon_0 c n_{ri} m^* L_{W,r}} \left\{ \sum_{j,f} f_{jf} \delta(E_{f,r} - E_{j,r} - \hbar\omega) (n_{s_{f,r}} - n_{s_{j,r}}) \right\} \right\rangle \quad (7)$$

$$\wp = \frac{\Gamma}{\pi [(\hbar\omega - (E_{f,r} - E_{j,r}))^2 + \Gamma^2]} \quad (8)$$

Here, N_W is the number of wells, ε_0 the absolute permittivity, c the velocity of light, n_{ri} the refractive index of the material, Γ the half-width at half-maxima, and $n_{s_{f,r}}$ and $n_{s_{j,r}}$ are the densities of two-dimensional electron gas in the f -th and j -th subband, respectively. The delta-function in Eq. (7) is replaced by the Lorentzian lineshape function (\wp) in Eq. (8) to obtain the absorption coefficient spectra of the non-uniform doped MQW structure under different design criteria as discussed in the next section.

3. RESULTS AND DISCUSSION

The absorption coefficient in a MQW structure is computed and plotted using Eq. (10). In Figure 2, absorption coefficient is plotted with wavelength (λ) for a 50-period $GaAs/Al_xGa_{1-x}As$ MQW structure at different well doping densities (N_D) keeping the contact layer doping density constant ($2.0 \times 10^{24} \text{ m}^{-3}$) at 77 K. It is seen from the plot that with increase of the well doping density, peak of the absorption

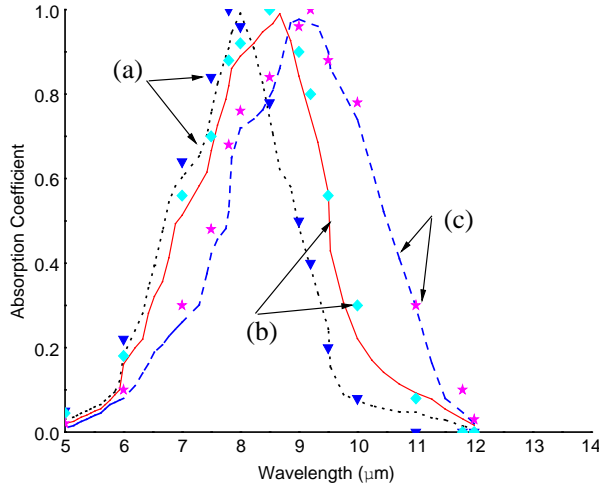


Figure 2. Plot of absorption coefficient vs. wavelength of a fifty-period $GaAs/Al_xGa_{1-x}As$ MQW structure with well doping density (N_D) as parameter at 77 K. (a) $N_D = 4.7 \times 10^{22} \text{ m}^{-3}$. (b) $N_D = 1.2 \times 10^{23} \text{ m}^{-3}$. (c) $N_D = 1.9 \times 10^{24} \text{ m}^{-3}$. The barrier width is 50 nm, well width is 4 nm and contact layer doping density is $2.0 \times 10^{24} \text{ m}^{-3}$. Symbols are used for experimental data taken from the literature in Ref. [10].

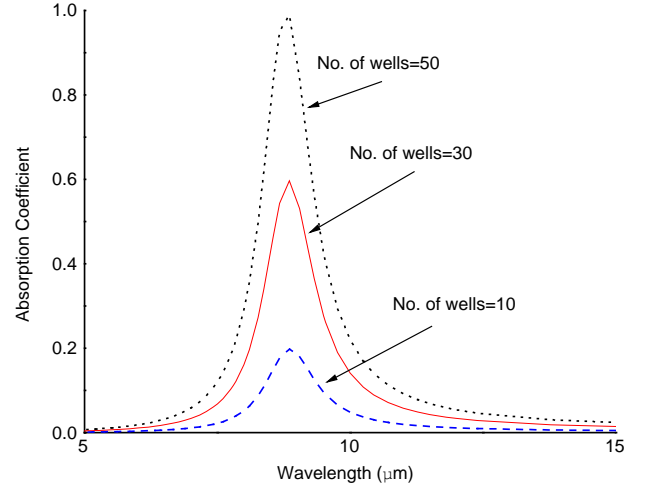


Figure 3. Variation of absorption coefficient with wavelength of a $GaAs/Al_xGa_{1-x}As$ MQW structure for different number of wells (NW). The width of the barrier and well layers are 50 nm and 4 nm respectively, well doping density is $1.2 \times 10^{23} \text{ m}^{-3}$ and $T = 77 \text{ K}$.

coefficient makes a red shift. Absorption at different wavelength of incident radiation reflects the relative change in the intersubband energy gap with the variation in the well doping density. The barrier width and well width are 50 nm and 4 nm respectively. Results show that theoretical findings manifests close agreement with the available experimental data [10].

The absorption coefficient is plotted as a function of wavelength in Figure 3 for different number of wells. The absorption coefficient curves for the 30- and 10-well structures are normalized with respect to the 50-wells MQW structure. It is seen that the magnitude of absorption coefficient peak increases with increase in the number of wells, which in turn enhances the full width half maximum (FWHM). Since a specific applied bias keeps intersubband energy constant the total absorption coefficient is the summation of absorption of photons in each well. Hence by adding more wells in the structure, probability of photon absorption increases, which makes the coefficient higher. One important observation can be made from the figure is that the peak position is invariant with respect to the wavelength.

Figure 4 shows the plot of absorption coefficient with wavelength for three different applied bias profile. With increase of field absorption coefficient peak shifts very slightly towards the shorter wavelength. This can be attributed to the infinitesimal increase in the separation between eigen energies in the quantum well with larger electric field. So, the absorption coefficient peak can be tuned to occur at the desirable operating wavelength by externally applied bias. This finding will play crucial role in designing photonic detectors using superlattice structures.

The results discussed so far are for the MQW structure with quantum wells of same doping density and thickness. Next, we study the effect of asymmetric and non-uniform well doping density on the absorption coefficient of the MQW structure. In Figure 5, it is observed that both the non-uniform asymmetric and non-uniform symmetric doping density distribution yields higher magnitude of absorption coefficient at the same corresponding wavelength than the uniform, symmetric structure. However, the absorption coefficient peak attains its maximum value when the wells of the MQW structure are doped in a non-uniform symmetric fashion. This can be explained as follows. The

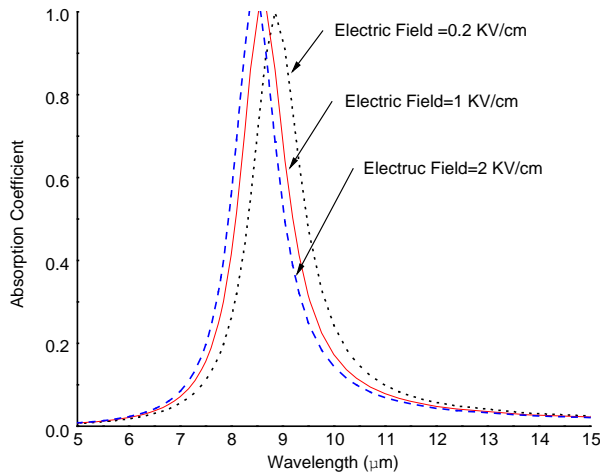


Figure 4. Absorption coefficient vs. wavelength of a 10-well $GaAs/Al_xGa_{1-x}As$ MQW structure at different applied bias which corresponds to the different values of electric field across the leftmost barrier adjacent to the emitter end. The width of the barrier and well layers are 50 nm and 4 nm respectively, well doping density is $1.2 \times 10^{23} \text{ m}^{-3}$ and $T = 77 \text{ K}$.

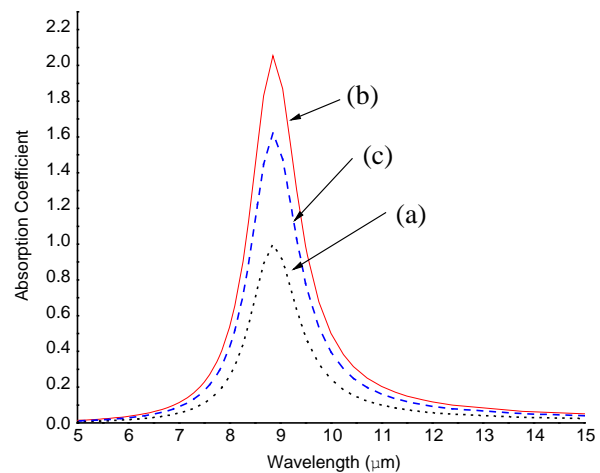


Figure 5. Absorption coefficient vs. wavelength of a $GaAs/Al_xGa_{1-x}As$ 10-well MQW structure for non-uniform and asymmetric well doping density. (a) Uniform and symmetric well doping density (N_D) = $1.2 \times 10^{23} \text{ m}^{-3}$. (b) Non-uniform symmetric well doping density (m^{-3}) = [4×10^{21} 6×10^{21} 4×10^{22} 6×10^{22} 1.2×10^{23} 1.2×10^{23} 6×10^{22} 4×10^{22} 6×10^{21} 4×10^{21}]. (c) Non-uniform asymmetric well doping density (m^{-3}) = [6×10^{21} 1.2×10^{22} 4×10^{22} 6×10^{22} 1.2×10^{23} 1.2×10^{23} 4×10^{23} 6×10^{23} 1×10^{24} 1.9×10^{24}]. The width of the barrier is 50 nm, well is 4 nm and T is 77K.

absorption coefficient is directly proportional to the subband density of electrons as can be understood from the formula. With the non-uniform variation of the doping density from one well to another well either in asymmetric or symmetric manner, the subband density of electrons increases compared to that of the uniform, symmetric MQW structure. Thus, the absorption of incident photons in such non-uniform symmetrically doped MQW structure is enhanced at the same operating wavelength which is beneficial for the detection of the weak signal.

The effect of non-uniform symmetric well width on the absorption coefficient characteristics is shown in Figure 6. Both types of non-uniformity (either gradually increasing outward or decreasing outward from the centre well) shift the absorption coefficient peak towards shorter wavelength, i.e., blue shift is observed. Again, the shifted peak of the absorption coefficient occurs at the identical wavelength for both the non-uniform symmetric MQW structures. The magnitude of the absorption coefficient peak yielded by the non-uniform symmetric structure where the well width decreases gradually outward from the centre well is higher than that of the uniform symmetric structure. The same is true also when the well width is increasing outward from the centre well. The average intersubband transition energy of both types of non-uniform symmetric MQW structures being the same, the blue-shifted absorption coefficient peak is exhibited at the identical wavelength by both these structures. The intersubband energy separation differs from one well to another well in the non-uniform symmetric MQW structure. Further, the variation of transition energy between subbands in each of the quantum wells in non-uniform symmetric MQW structure with well widths gradually decreasing outward from centre well is non-identical with that in the non-uniform symmetric MQW structure with well widths gradually increasing outward from the centre well. Hence, these two types of non-uniform symmetric MQW structures show remarkable difference in the magnitude of the blue-shifted absorption coefficient peaks. However, the average oscillator strength of intersubband transitions in each of the non-uniform symmetric MQW structures is responsible for the higher magnitude of the absorption coefficient peaks with respect to that of the uniform symmetric structure.

In Figure 7, the effect of non-uniform asymmetric dimensional distribution of well layers on the absorption coefficient vs. wavelength characteristics of MQW structures is studied. Both the non-

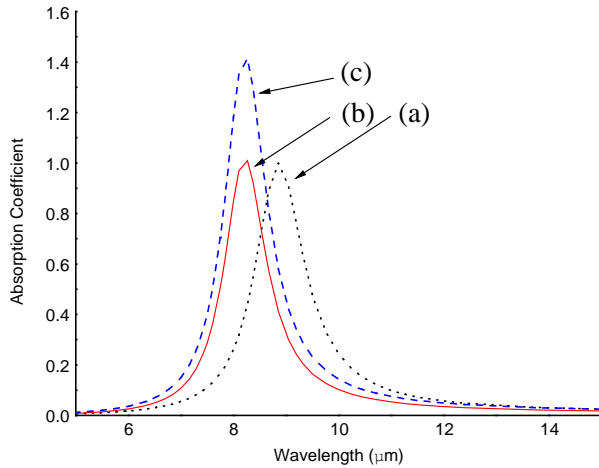


Figure 6. Absorption coefficient vs. wavelength characteristics of a $GaAs/Al_xGa_{1-x}As$ MQW (ten wells) structure with non-uniform well width. (a) Uniform symmetric well width = 4 nm. (b) Non-uniform symmetric well width (nm) = [5.6 5.2 4.8 4.4 4 4 4.4 4.8 5.2 5.6]. (c) Non-uniform symmetric well width (nm) = [4 4.4 4.8 5.2 5.6 5.6 5.2 4.8 4.4 4]. Barrier width = 50 nm, well doping density = $1.2 \times 10^{23} \text{ m}^{-3}$ and T is 77 K.

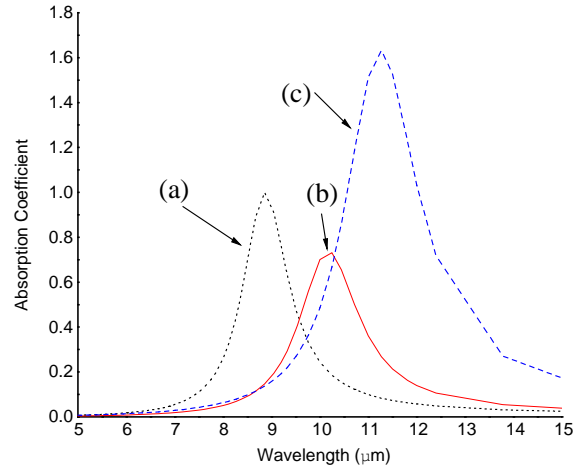


Figure 7. Absorption coefficient vs. wavelength characteristics of a $GaAs/Al_xGa_{1-x}As$ MQW (ten wells) structure with non-uniform asymmetric well width. (a) Uniform symmetric well width = 4 nm. (b) Non-uniform asymmetric well width (nm) = [5.6 5.2 4.8 4.4 4 4 3.6 3.2 2.8 2.4]. (c) Non-uniform asymmetric well width (nm) = [2.4 2.8 3.2 3.6 4 4 4.4 4.8 5.2 5.6]. Barrier width = 50 nm, well doping density = $1.2 \times 10^{23} \text{ m}^{-3}$ and T is 77 K.

uniform asymmetric MQW structures, with well widths either decreasing or increasing gradually from the emitter end towards the collector end, exhibit red shift of absorption coefficient peak. The coefficient is reduced in the non-uniform asymmetric MQW structure with decreasing well width compared to that of the uniform symmetric structure. On the contrary, it is seen that the absorption coefficient rises significantly in the non-uniform asymmetric MQW structure where well width increases gradually from the left towards the right contact end. The averages of the intersubband transition energy being different for both types of asymmetric structures, their absorption coefficient peak positions also vary with wavelength. The absorption coefficient peak is diminished in asymmetric structure with well widths decreasing from left towards right contact region due to the fact that the average oscillator strength of intersubband transition in this structure is less than that of the uniform symmetric structure. However, the average oscillator strength in asymmetric structure where well width increases gradually from the emitter side to the collector layer being greater than that of the uniform symmetric structure yields noticeably large absorption coefficient peak. So, the incorporation of non-uniformity in distributing well layer thickness causes either blue-shift or red-shift of coefficient peak along with reduction or enhancement of its magnitude respectively. This may be useful for the absorption of large number of incident photons along with the tuning of the wavelength selectivity of the intersubband photodetectors in the infra red (IR) range.

The influence of non-uniform well doping density along with non-uniform symmetric and asymmetric well thickness is computed and plotted in Figure 8 and Figure 9 respectively. When the distribution pattern of quantum well doping density is non-uniform symmetric with well width non-uniformity of either symmetry (Figure 8) or asymmetry (Figure 9) the absorption coefficient peak

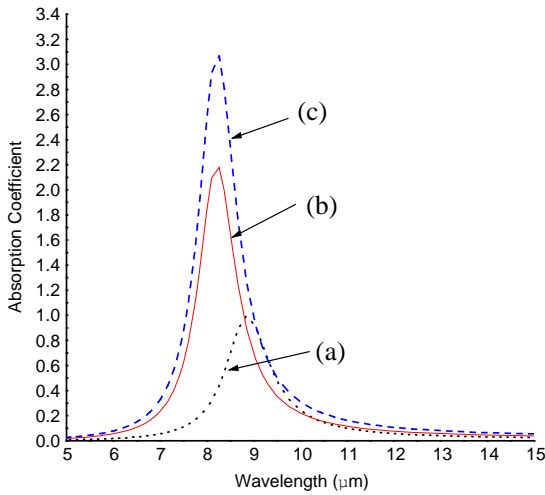


Figure 8. Absorption coefficient vs. wavelength characteristics of a $GaAs/Al_xGa_{1-x}As$ MQW (ten wells) structure with non-uniform well width and doping density. (a) Uniform and symmetric well doping density (N_D) = $1.2 \times 10^{23} \text{ m}^{-3}$, well width = 4 nm. (b) Non-uniform symmetric well doping density (m^{-3}) = $[4 \times 10^{21} \ 6 \times 10^{21} \ 4 \times 10^{22} \ 6 \times 10^{22} \ 1.2 \times 10^{23} \ 1.2 \times 10^{23} \ 6 \times 10^{22} \ 4 \times 10^{22} \ 6 \times 10^{21} \ 4 \times 10^{21}]$, well width (nm) = $[5.6 \ 5.2 \ 4.8 \ 4.8 \ 4.4 \ 4 \ 4 \ 4.4 \ 4.8 \ 5.2 \ 5.6]$. (c) Non-uniform symmetric well doping density (m^{-3}) = $[4 \times 10^{21} \ 6 \times 10^{21} \ 4 \times 10^{22} \ 6 \times 10^{22} \ 1.2 \times 10^{23} \ 1.2 \times 10^{23} \ 6 \times 10^{22} \ 4 \times 10^{22} \ 6 \times 10^{21} \ 4 \times 10^{21}]$, well width (nm) = $[4 \ 4.4 \ 4.8 \ 5.2 \ 5.6 \ 5.6 \ 5.2 \ 4.8 \ 4.4 \ 4]$. Barrier width = 50 nm and T is 77 K.

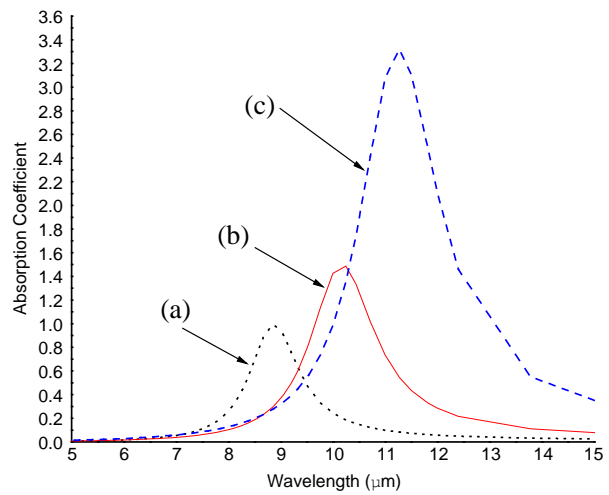


Figure 9. Absorption coefficient vs. wavelength characteristics of a $GaAs/Al_xGa_{1-x}As$ MQW (ten wells) structure with non-uniform well width and doping density. (a) Uniform and symmetric well doping density (N_D) = $1.2 \times 10^{23} \text{ m}^{-3}$, well width = 4 nm. (b) Non-uniform symmetric well doping density (m^{-3}) = $[4 \times 10^{21} \ 6 \times 10^{21} \ 4 \times 10^{22} \ 6 \times 10^{22} \ 1.2 \times 10^{23} \ 1.2 \times 10^{23} \ 6 \times 10^{22} \ 4 \times 10^{22} \ 6 \times 10^{21} \ 4 \times 10^{21}]$, asymmetric well width (nm) = $[5.6 \ 5.2 \ 4.8 \ 4.8 \ 4.4 \ 4 \ 4 \ 3.6 \ 3.2 \ 2.8 \ 2.4]$. (c) Non-uniform symmetric well doping density (m^{-3}) = $[4 \times 10^{21} \ 6 \times 10^{21} \ 4 \times 10^{22} \ 6 \times 10^{22} \ 1.2 \times 10^{23} \ 1.2 \times 10^{23} \ 6 \times 10^{22} \ 4 \times 10^{22} \ 6 \times 10^{21} \ 4 \times 10^{21}]$, asymmetric well width (nm) = $[2.4 \ 2.8 \ 3.2 \ 3.6 \ 4 \ 4 \ 4.4 \ 4.8 \ 5.2 \ 5.6]$. Barrier width = 50 nm and T is 77 K.

attains significantly higher magnitude compared to that of the uniform symmetric structure as well as the non-uniform symmetric or asymmetric MQW structure shown in Figure 6 and Figure 7 respectively. The reason for this phenomenon is already well understood from the explanation of Figure 5. Hence, the non-uniform distribution of well doping density along with structural parameters of the MQW intersubband photodetector can be preferred to increase the absorption of incident photons even when the incident radiation strength is relatively low.

4. CONCLUSION

The absorption coefficient characteristics are theoretically investigated for uniform, non-uniform symmetric and non-uniform asymmetric distribution of well thickness and well doping density in MQW intersubband photodetector. Increase of absorption coefficient with increase in the number of wells is inferred from the mathematical formulae and is also manifested in the results. Electrical tuning of absorption coefficient peak is possible by externally applied field along the quantized direction. Further, it is noticed that the non-uniform doping density distribution where it decreases gradually from the centre well of the MQW structure yields remarkably larger absorption coefficient peak compared to the uniform symmetric doped and also asymmetric doped MQW structure. The doped non-uniform symmetric MQW structure (in terms of well thickness) exhibits the blue-shift of absorption coefficient peak whereas red-shift is shown by the doped non-uniform asymmetric MQW structure. Interestingly, the incorporation of non-uniformity of quantum well doping density distribution along with the well layer thickness significantly increases the magnitude of the absorption coefficient peak than that of the uniform symmetric structure at the required operating wavelength. Hence, appropriate tuning of structural parameters in terms of non-uniform well doping density is preferred for the detection of weak signals along with the non-uniform symmetric or asymmetric distribution of well layer thickness that is found suitable for the tuning of wavelength selectivity.

ACKNOWLEDGMENT

The work was financially supported partially by the Council of Scientific & Industrial Research (CSIR), India under the Senior Research Fellowship scheme.

REFERENCES

1. Manasreh, M. O., *Semiconductor Quantum Wells and Superlattices for Long-wavelength Infrared Detectors*, Artech House, Boston, MA, 1993.
2. Davies, J. H., *The Physics of Low-dimensional Semiconductors: An Introduction*, Cambridge University Press, Cambridge, 1998.
3. Basu, P. K., *Theory of Optical Processes in Semiconductors: Bulk and Microstructures*, Clarendon Press, 2003.
4. Levine, B. F., "Quantum-well infrared photodetectors," *Journal of Applied Physics*, Vol. 74, No. 8, R1, 1993.
5. Cen, L. B., B. Shen, Z. X. Qin, and G. Y. Zhang, "Near-infrared two-color intersubband transitions in AlN /GaN coupled double quantum wells," *Journal of Applied Physics*, Vol. 105, No. 5, 053106, 2009.
6. Jdidi, A., N. Sfina, S. A. Nassrallah, M. Said, and J. L. Lazzari, "A multi-color quantum well photodetector for mid- and long-wavelength infrared detection," *Semiconductor Science & Technology*, Vol. 26, No. 12, 125019, 2011.
7. Fauci, M. A., R. Breiter, W. Cabanski, W. Fick, R. Koch, J. Zeigler, and S. D. Gunapala, "Medical infrared imaging — Differentiating facts from fiction, and the impact of high precision quantum well infrared photodetector camera systems, and other factors, in its reemergence," *Infrared Physics & Technology*, Vol. 42, Nos. 3–5, 337–344, 2001.

8. Eker, S. U., M. Kaldirim, Y. Arslan, and C. Besikci, "Large-format voltage-tunable dual-band quantum-well infrared photodetector focal plane array for third-generation thermal imagers," *IEEE Electron Device Letters*, Vol. 29, No. 10, 1121–1123, 2008.
9. Zhou, T., R. Zhang, X. G. Guo, and Z. Y. Tan, "Terahertz imaging with quantum well photodetectors," *IEEE Photonics Technology Letters*, Vol. 24, No. 13, 1109–1111, 2012.
10. Gunapala, S. D., B. F. Levine, L. Pfeiffer, and K. West, "Dependence of the performance of GaAs/AlGaAs quantum well infrared photodetectors on doping and bias," *Journal of Applied Physics*, Vol. 69, No. 9, 6517–6520, 1991.
11. Yang, Y., H. C. Liu, W. Z. Shen, N. Li, W. Lu, Z. R. Wasilewski, and M. Buchanan, "Optimal doping density for quantum-well infrared photodetector performance," *IEEE Journal of Quantum Electronics*, Vol. 45, No. 6, 623–628, 2009.
12. Steele, A. G., H. C. Liu, M. Buchanan, and Z. R. Wasilewski, "Importance of the upper state position in the performance of quantum well intersubband infrared detectors," *Applied Physics Letters*, Vol. 59, No. 27, 3625–3627, 1991.
13. Steele, A. G., H. C. Liu, M. Buchanan, and Z. R. Wasilewski, "Influence of the number of wells in the performance of multiple quantum well intersubband infrared detectors," *Journal of Applied Physics*, Vol. 72, No. 3, 1062–1064, 1992.
14. Liu, H. C., G. C. Aers, M. Buchanan, Z. R. Wasilewski, and D. Landheer, "Intersubband photocurrent from the quantum well of an asymmetrical double-barrier structure," *Journal of Applied Physics*, Vol. 70, No. 2, 935–940, 1991.
15. Ting, D. Z.-Y., C. J. Hill, A. Soibel, S. A. Keo, J. M. Mumolo, J. Nguyen, and S. D. Gunapala, "A high-performance long-wavelength superlattice complementary barrier infrared detector," *Applied Physics Letters*, Vol. 95, No. 2, 023508, 2009.
16. Machhadani, H., Y. Kotsar, S. Sakr, M. Tchernycheva, R. Colombelli, J. Mangeney, E. Bellet-Amalric, E. Sarigiannidou, E. Monroy, and F. H. Julien, "Terahertz intersubband absorption in GaN/AlGaN step quantum wells," *Applied Physics Letters*, Vol. 97, No. 19, 191101, 2010.
17. Manasreh, O., *Semiconductor Heterojunctions and Nanostructures*, McGraw-Hill, New York, 2005.